Study of Wave Propagation Anomalies at Deception Island Volcano by Using Numerical Simulations and Array Techniques

Autora: Itahisa González Álvarez
Director: Dr. Javier Almendros González

MÁSTER GEOMET
Universidad de Granada
Curso 2015 - 2016

Abstract. The propagation of seismic waves in volcanic environments is usually affected by their typical sharp topographies as well as by multiple kinds of heterogeneities in the medium they propagate through. García Yeguas *et al.* (2011) found important wave propagation anomalies at Deception Island volcano, which were hypothesised as the effect of topography and velocity structure over the propagating waves. In this work, a realistic model including both the velocity structure of Deception Island and its topography was used for a series of numerical simulations in order to find out whether their anomalous results were caused by the combined effect of the topography and the velocity structure. Our results prove the accuracy and usefulness of numeric simulations and confirm García Yeguas *et al.* (2011) initial hypothesis.

Keywords: seismic array, wave propagation, numerical simulation, Deception Island, azimuth anomaly, apparent slowness

INTRODUCTION

The propagation of seismic waves in volcanic environments is usually affected by their typical sharp topographies as well as by multiple kinds of heterogeneities that cause them to attenuate, deviate from their initial path and/or change their velocity (and, consequently, to alter their traveltime). The study of such waves allows to obtain valuable information about the inner structure of the volcano and its dynamics (e.g. Kumagai and Chouet, 1999; Chouet *et al.*, 2003; Di Grazia *et al.*, 2009; Patanè *et al.*, 2006; 2013). For example, traveltime tomography uses the delays induced on P and S waves by those heterogeneities to characterize the velocity structure of the area (e.g. Zandomeneghi*et al.* 2009).

Seismic arrays, or seismic antennas, are defined as a group of similar and syncronized seismic stations arranged in a geometric pattern over a homogeneous area. By comparing the seismograms registered at each individual station, seismic arrays allow to estimate temporal and spatial variations of the propagation properties (usually direction and apparent velocity in the form of the apparent slowness vector) of the waves propagating across the array. Combining several of them can be even more advantageous, as this technique provides also information about the position of the source. As array methods do not require seismic waves to contain clearly differentiated phases, they are an essential tool for volcanic seismicity studies, where seismic signals do not usually show them (e.g., Almendros *et al.*, 1997).

In 2005, an active-source tomographic experiment was carried out at Deception Island volcano (South Shetland Islands, Antarctica). For that purpose, more than 6000 air gun shots were

fired all around the island (including Port Foster, the central bay at its centre), generating seismic waves in the process which were registered by both land and ocean bottom seismometers deployed on and around the island. Those seismic stations were arranged both as individual stations and as part of dense and sparse seismic arrays located along the inner coast of Port Foster. From those high-quality data, Zandomeneghi *et al.* (2009) obtained a high-resolution velocity model of the island and García Yeguas *et al.* (2011) studied the propagation of the seismic waves across the heterogenous medium of the volcano.

Eight of the aforementioned arrays were used by García Yeguas *et al.* (2011) to estimate the apparent slowness vectors of the wavefields generated by the air-gun shots. Since the shot locations were known, they were able to study the wave propagation in detail. Thus, they found important wave propagation anomalies which were hypothesised as being the effect of the velocity structure of the island. These results showed the necessity of taking local velocity structure, topography and bathymetry into account, especially for classical seismology methods, where oversimplified models have been traditionally used, thus ignoring the complexity and heterogeneity of volcanic structures. These authors also pointed out the advantages of modern computational methods, which are capable of effectively including the effects of topography as well as precise velocity structure models in order to perform more accurate simulations of waves propagation.

In the work presented here, I will carry on a series of simulations in order to find out whether the anomalous results obtained by García Yeguas *et al.* in 2011 were caused by the combined effect of the topography and the velocity structure.

Tomodec Experiment

In January 2005, TOMODEC project, an active source tomographic experiment, was carried out at Deception Island volcano. The main aim of TOMODEC was to obtain a tomographic image of Deception Island and its surroundings, but gravity, magnetic and bathymetry data were also acquired (Barclay *et al.*, 2009; Zandhomenegi *et al.*, 2009).

The apparent slowness vectors of the first arrivals of the seismic waves generated by the air gun shots during TOMODEC experiment were calculated by García Yeguas *et al.* (2011) by using the Zero Lag Cross Correlation (ZLCC) method, which looks for the maximum array-average cross-correlation values of the aligned waveforms within an apparent slowness grid. Seismic arrays methods provide apparent slowness vectors, representing the direction (as the propagation angle measured from north or azimuth) and apparent velocity (or apparent slowness, its inverse) of seismic waves travelling across the array. Their analysis of both azimuth and apparent slowness data at eight different arrays showed anomalies at some of them, in the form of wave fronts propagating in directions different from the shot-array directions in some areas or faster in some directions (thus generating asymmetric wave fronts, instead of radially symmetric ones). In general, positive anomalies appeared in larger and more conspicuous areas than negative ones, being this the most prominent feature. Moreover, it is also remarkable the absence of radial symmetry in the apparent slowness values, shown in the form of shots at similar distances from the array yielding different apparent slowness values. Specifically, figure 1a contains García Yeguas *et al.* (2011) results for azimuth anomaly at each array, defined as the difference between the orientation of the estimated apparent slowness vector and the geometrical azimuth from the shot position to the array centre. Thus, positive values of the azimuth anomaly represent a clockwise rotation of the apparent slowness vector, while small negative anomaly values correspond to counterclockwise rotations. These results, showing several regions where the wavefronts propagate in directions different from the shot-array direction, are interpreted as an illustration of the influence of the medium in wave propagation. Some of them coincide with the hypothesised magma chamber beneath the northern sector of Port Foster, but this feature is not enough to explain all the observed anomalies, which

were interpreted as the effect of additional lateral heterogeneities over the ray path.

Method and data processing

The original air-gun shots were simulated by means of the finite-difference method, which numerically solve differencial equations by approximating the derivatives with finite differences. In this case, the wave propagation equations are solved by using a finely discretized space and small time steps, so that derivatives can be approximated by ratios of differences (e.g. Virieux and Madariaga, 1982). The version of the finite-difference method used for this work was developed by Ohmninato and Chouet in 1997, its main purpose being evaluating the effect of 3D topography on wave propagation in volcanic areas. In the work presented here, the simulations were carried on on a realistic medium which includes Deception Island's topography, bathymetry and 3D velocity structure (obtained by Zandomeneghi *et al.* (2009)).

The results obtained from the finite-difference method were analysed using the Zero Lag Cross Correlation (ZLCC) method (Frankel *et al.* 1991; Del Pezzo *et al.* 1997; Almendros *et al.* 1999). It consists on evaluating every possible value of the apparent slowness within a grid in order to maximize the average cross-correlation coefficient. The application of this method implies the assumption of a homogeneous medium below the array, a wavefield composed only of plane waves and the random character of the noise, which would make null its correlation with the signal.

Results

Figure 1 shows the azimuth anomaly results for 1 and 2 Hz sources respectively, comparing those results obtained from P-wave detection data and those from surface waves data. A large positive anomaly area appears to the north of Port Foster, with azimuth anomaly magnitude reaching 20 degrees (this meaning a 20 degrees clockwise rotation of the apparent slowness vector from the shot-array direction). Another positive anomaly area to the southeast of the bay is also present in all these graphs, its magnitude much lower than that of the large one. The negative anomaly area in the vicinity of the array is also a common feature, with up to 30 degrees apparent slowness vectors counterclockwise rotations. The more "detailed" distribution obtained for 2 Hz sources, which indicates a stronger effect of the topography and velocity structure over their propagation than over the 1 Hz ones.

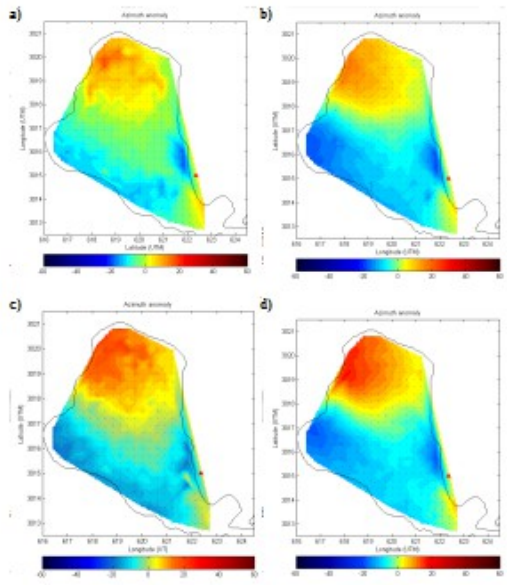

Figure 1. Azimuth anomaly distribution for 1 Hz (a and b) and 2Hz sources (c and d). Graphs a and c contain the results obtained from P-wave data, while b and d show those from surface waves data.

Figure 2 compares the apparent slowness results obtained for 1 and 2 Hz sources and P-wave and surface waves data. However, these distributions are not as similar among them as the azimuth anomaly ones were. Again, 2 Hz sources show more variations of apparent slowness (therefore, a greater effect of the topography and velocity structure) than the 1 Hz ones, but the remaining distribution seems to coincide in all four graphs except for the apparent slowness magnitude, which is naturally higher for surface waves as they move slower than P-waves. For 1 Hz sources, there seems to be some kind of artifact to the South of the array, both for P-wave and surface waves. As it is explained in section 4.2., it was not possible to separate the arrival of P-waves from that of surface waves for these sources, therefore the abnormal distribution and

magnitude of apparent slowness in this area.

As this study has tried to replicate the results obtained by García Yeguas *et al.* (2011), a final comparison between experimental and synthetic apparent slowness and azimuth anomaly results is required. In order to facilitate it, Figure 3 displays the original results by García Yeguas *et al.* (2011) for P-wave azimuth anomaly and apparent slowness next to the same results obtained for 2 Hz sources from these simulations. The colour map has been changed here in order to make both graphs look as similar as possible. Apparent slowness results show great similarity with García Yeguas *et al.* (2011) data, both in distribution and magnitude. Lower values of apparent slowness appear around northwestern Port Foster, thus agreeing both with experimental and tomographic data, as this is where the low velocity region was located in the tomographic data. Nearby shots, however, produce larger apparent slowness values, especially those located around the high velocity area to the south of the array. From the observation of the seismograms of some of the sources, it is also possible to see a correlation between the observed differences and singularities along the different profiles and the changes in apparent slowness. Tthere are several small regions with different values of apparent slowness that approximately coincide with the positions of the sources showing changes in their seismograms.

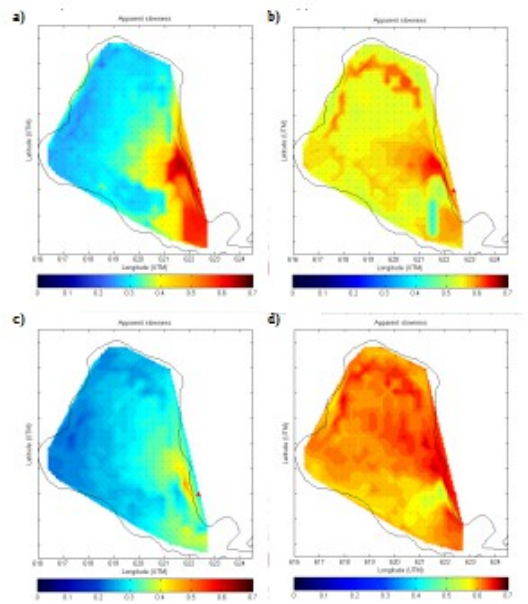

Figure 2. Apparent slowness distributions for 1 Hz (a and b) and 2 Hz (c and d) sources. As in Figure 20, left graphs (a and c) show the results for P-wave, while the right ones contain those for surface waves (c and d). Note that different color scales have been used for P-wave and surface waves graphs in order to facilitate the visualization of variations in the apparent slowness magnitude.

Azimuth anomaly results are also very similar to the experimental ones. The large positive azimuth anomaly region to the north of Port Foster (meaning that rays with origin within this region deviate from the source-to-array direction clockwise) seem to be located right above the low velocity area while the negative anomaly region on southwestern Port Foster seem to indicate that seismic rays travel around the hypothesised magma chamber (thus being deviated counterclockwise from the path they would follow on a homogeneous medium) on their way to the array. Again, the observed differences along the profiles coincide with marked differences on azimuth anomalies.

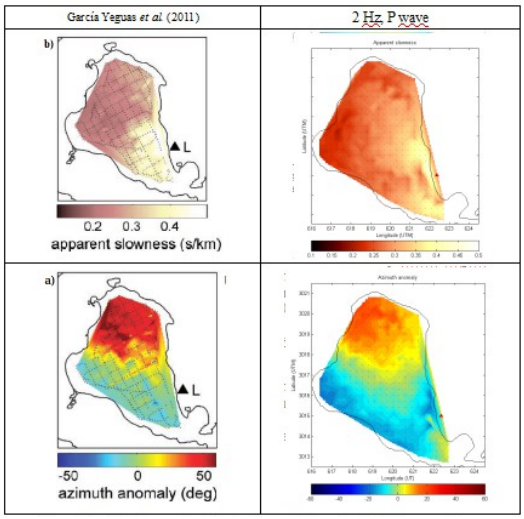

Figure 3. On the left, graphical display of García Yeguas et al. (2011) apparent slowness and azimuth anomaly data. Synthetic results are shown on the right for 2 Hz sources. Both colormap and scale have been set to resemble the original diagrams and make comparisons easier.

CONCLUSIONS

Heterogeneities and sharp topographies have been traditionally neglected in volcanic seismicity studies in order to apply simpler calculation methods but it is necessary (and possible) to consider more realistic mediums.

García Yeguas *et al.* (2011) found important wave propagation anomalies which were hypothesised as the result of topography and velocity structure. In this work, a realistic domain

including both the velocity structure of Deception Island and its topography (both of them acknowledging the presence of the ocean around the island) was applied for our simulations. Apparent slowness vectors results can vary greatly depending on even small variations of the position of the source, thus the importance of using an accurate velocity model for array studies.

The limitations of our method and the resolution of both the topography and tomography data did not allow to recreate the original sources more accurately, as only frequencies up to 2 Hz were possible and the original sources had spectra centred at 6 Hz. The analysis of sources located near the array showed some problems, especially at low frequencies. One of the requirements of the ZLCC method was that the wavefield would be composed by plane waves only. However, for sources near the array, the curvature of the wavefronts can not be ignored and may have produced the observed anomalous results. Still, the obtained distributions of apparent slowness and azimuth anomaly within Port Foster coincide greatly with those of García Yeguas *et al.* (2011), thus demonstrating that their results were produced by a combined effect of the topography and the velocity structure. It is also convenient to note that seismic waves generated by higher frequency sources are more affected by sharp topographies and heterogeneities than those with lower frequencies, thus implying that the observed differences between the results on figure 22 and those of García Yeguas *et al.* (2011) could be due to differences between the frequency content of their respective sources. Moreover, it would be reasonable to expect even more similar results by using synthetic sources with higher frequencies.

REFERENCES

1. Almendros, J., Ibáñez, J. M., Alguacil, G., Del Pezzo, E., & Ortiz, R. (1997). Array tracking of the volcanic tremor source at Deception Island, Antarctica. *Geophysical Research Letters*, *24*(23), 3069-3072.
2. Almendros, J., Ibáñez, J. M., Alguacil, G., & Del Pezzo, E. (1999). Array analysis using circular-wave-front geometry: an application to locate the nearby seismo-volcanic source. *Geophysical Journal International*, *136*(1), 159-170.
3. Barclay, A. H., Wilcock, W. S. D., & Ibáñez, J. M. (2009). Bathymetric constraints on the tectonic and volcanic evolution of Deception Island Volcano, South Shetland Islands. *Antarctic Science*, *21*(02), 153-167.
4. Chouet, B., Dawson, P., Ohminato, T., Martini, M., Saccorotti, G., Giudicepietro, F., ... & Scarpa, R. (2003). Source mechanisms of explosions at Stromboli Volcano, Italy, determined from moment-tensor inversions of very-long-period data. *Journal of Geophysical Research: Solid Earth*, *108*(B1).
5. Del Pezzo, E., La Rocca, M., & Ibanez, J. (1997). Observations of high-frequency scattered waves using dense arrays at Teide volcano. *Bulletin of the Seismological Society of America*, *87*(6), 1637-1647.
6. Di Grazia, G., Cannata, A., Montalto, P., Patanè, D., Privitera, E., Zuccarello, L., & Boschi, E. (2009). A multiparameter approach to volcano monitoring based on 4D analyses of seismo-volcanic and acoustic signals: The 2008 Mt. Etna eruption. *Geophysical Research Letters*, *36*(18).
7. Frankel, A., Hough, S., Friberg, P., & Busby, R. (1991). Observations of Loma Prieta aftershocks from a dense array in Sunnyvale, California. *Bulletin of the seismological Society of America*, *81*(5), 1900-1922.
8. García Yeguas, A., Almendros, J., Abella, R., & Ibáñez, J. M. (2011). Quantitative analysis of seismic wave propagation anomalies in azimuth and apparent slowness at Deception Island volcano (Antarctica) using seismic arrays. *Geophysical Journal International*, *184*(2), 801-815.
9. Kumagai, H., & Chouet, B. A. (1999). The complex frequencies of long-period seismic events as probes of fluid composition beneath volcanoes. *Geophysical Journal International*, *138*(2), F7-F12.
10. Ohminato, T., & Chouet, B. A. (1997). A free-surface boundary condition for including 3D topography in the finite-difference method. *Bulletin of the Seismological Society of America*, *87*(2), 494-515.
11. Patanè, D., Barberi, G., Cocina, O., De Gori, P., & Chiarabba, C. (2006). Time-resolved seismic tomography detects magma intrusions at Mount Etna. *Science*, *313*(5788), 821-823.
12. Patanè, D., Aiuppa, A., Aloisi, M., Behncke, B., Cannata, A., Coltelli, M., ... & Salerno, G. (2013). Insights into magma and fluid transfer at Mount Etna by a multiparametric approach: a model of the events leading to the 2011 eruptive cycle. *Journal of Geophysical Research: Solid Earth*, *118*(7), 3519-3539.
13. Virieux, J., & Madariaga, R. (1982). Dynamic faulting studied by a finite difference method. *Bulletin of the Seismological Society of America*, *72*(2), 345-369.
14. Zandomeneghi, D., Barclay, A., Almendros, J., Ibáñez Godoy, J. M., Wilcock, W. S., & Ben-Zvi, T. (2009). Crustal structure of Deception Island volcano from P wave seismic tomography: Tectonic and volcanic implications. *Journal of Geophysical Research: Solid Earth*, *114*(B6).